Accretion Product Formation from Ozonolysis and OH Radical Reaction of α-Pinene: Mechanistic Insight and the Influence of Isoprene and Ethylene

Torsten Berndt,[*,#] Bernhard Mentler, [§] Wiebke Scholz,[§] Lukas Fischer,[§] Hartmut Herrmann,[#] Markku Kulmala,[⊥] and Armin Hansel[§]

[#] Atmospheric Chemistry Department (ACD), Leibniz Institute for Tropospheric Research (TROPOS), 04318 Leipzig, Germany.

[§]Institute for Ion Physics and Applied Physics, University of Innsbruck, 6020 Innsbruck, Austria.

[⊥] Institute for Atmospheric and Earth System Research (INAR) / Physics, University of Helsinki, Helsinki 00014, Finland.

[*] To whom correspondence should be addressed. E-mail: berndt@tropos.de

Abstract

α-Pinene, $C_{10}H_{16}$, represents one of the most important biogenic emissions in the atmosphere. Its oxidation products can significantly contribute to the secondary organic aerosol (SOA) formation. Here, we report on the formation mechanism of C_{19} and C_{20} accretion products from α-pinene oxidation, which are believed to be efficient SOA precursors. Measurements have been performed in a free-jet flow system. Detection of RO_2 radicals and accretion products was carried out by recent mass spectrometric techniques using different ionization schemes. Observed C_{10}-RO_2 radicals from α-pinene ozonolysis were O,O-$C_{10}H_{15}(O_2)_xO_2$ with x = 0, 1, 2, 3 and from the OH radical reaction HO-$C_{10}H_{16}(O_2)_\alpha O_2$ with α = 0, 1, 2. All detected C_{20} accretion products can be explained via the accretion reaction $RO_2 + R'O_2 \rightarrow ROOR' + O_2$ starting from the measured C_{10}-RO_2 radicals. We speculate that C_{19} accretion products are formed in an analogous way assuming CH_2O elimination. Addition of isoprene, C_5H_8, producing C_5-RO_2 radicals, leads to C_{15} accretion products formed via cross-reactions with C_{10}-RO_2 radicals. This process is competing with the formation of C_{19}/C_{20} products from the pure α-pinene oxidation. A similar behavior has been observed for ethylene additives that form C_{12} accretion products. In the atmosphere a complex accretion product spectrum from self- and cross-reactions of available RO_2 radicals can be expected. Modeling atmospheric conditions revealed that C_{19}/C_{20} product formation is only reduced by a factor of 1.2 or 3.6 in isoprene-dominated environments assuming a 2-fold or 15-fold isoprene concentration over α-pinene, respectively, as present in different forested areas.

Introduction

Monoterpenes, $C_{10}H_{16}$, are emitted into the atmosphere with a mean global rate of 95×10^6 metric tons of carbon per year. α-Pinene, the main $C_{10}H_{16}$ compound, accounts for about one-third of that.[1,2] Its atmospheric degradation, starting with the attack of hydroxyl (OH) or nitrate (NO_3) radicals or ozone (O_3) and subsequent O_2 addition, generates different RO_2 radicals as reactive intermediates.[3] These RO_2 radicals can undergo isomerization reactions, such as intra-molecular H shifts[4-8] or endo-cyclization in the case of unsaturated RO_2 radicals [7,9,10], which result in higher oxidized RO_2 radicals after subsequent O_2 addition. Competing bimolecular RO_2 radical reactions with NO, HO_2 or other RO_2 radicals as well as the RO_2 self-reaction represent the main loss processes in the atmosphere.[3]

It is well established that RO_2 self- and cross-reactions mainly form either the corresponding alkoxy radicals or an alcohol along with a carbonylic substance.[11-13] A third reaction pathway leading to peroxides, pathway (1), has been considered to be minor based on experimental results obtained from small RO_2 radicals such as CH_3O_2 or $C_2H_5O_2$.[14,15]

$$RO_2 + R'O_2 \rightarrow ROOR' + O_2 \quad (1)$$

In the course of investigations on atmospheric autoxidation processes and associated with the progress of analytical techniques in recent years, high-molecular weight products have been identified that are likely formed via the peroxide route according to pathway (1).[5-8,16-19] Very recently, universal validity of accretion product formation from the self- and cross-reactions of RO_2 radicals via pathway (1) has been proposed.[20]

Due to their lower vapor pressure, accretion products ROOR′ formed from C_{10}-RO_2 radicals of the α-pinene oxidation are believed to be more efficient aerosol precursors than the corresponding C_{10} closed-shell products.[21,22] For example, calculated vapor pressures of C_{20} accretion products from the OH + α-pinene reaction were below 10^{-15} atm while those of the corresponding highly oxidized C_{10} closed-shell products were in the range $(0.5 - 8) \times 10^{-10}$ atm.[7]

α-Pinene emissions in forestlands are accompanied by emissions of a series of other hydrocarbons, such as isoprene and ethylene, which are present in large excess over the monoterpenes in some areas.[23-25] For instance in the Amazon tropical forest, α-pinene mixing ratios are in the range of 0.05 - 0.15 ppbv, those of isoprene 1.14 - 2.72 ppbv and those of ethylene 0.63 - 1.68 ppbv.[23] It can be supposed that RO_2 radicals arising from the degradation of other hydrocarbons can significantly disturb the formation of pure α-pinene derived accretion products through competitive RO_2 cross-reactions. In this context, rates of early particle growth by organics, as experimentally determined for highly oxidized products from the pure α-pinene oxidation [26], do not hold describing field observations in isoprene-dominated forests.[27]

While different groups consistently observed the formation of C_{19} and C_{20} accretion products from α-pinene oxidation up to now [5-7,18,19,22,26], the knowledge on the mechanism, the reacting RO_2 radicals and the kinetics of this process is very sparse. Here, we use a free-jet flow system for mechanistic and kinetic studies of accretion product formation from α-pinene oxidation at close to atmospheric conditions. RO_2 radicals and closed-shell products are measured simultaneously applying most recent mass spectrometric techniques that provide a more complete overview of the product distribution. Isoprene and ethylene additives to the reaction gas gave insight into competing RO_2 radical reactions and the resulting modification of the product distribution.

Methods

The investigations were carried out in a free-jet flow system at a temperature of 297 ± 1 K and a pressure of 1 bar purified air that allows experiments for almost wall-free conditions.[7,20,28] Briefly, the flow system consists of an outer tube (i.d. 16 cm, length of 200 cm) and an inner tube (o.d. 9.5 mm) equipped with a nozzle. The first reactant, usually ozone, premixed with air (5 L min^{-1} STP) is injected through the inner tube into the main gas stream (95 L min^{-1} STP), which contains the second reactant, α-pinene and other organics if needed. The chosen flow conditions and the nozzle geometry ensure rapid reactant mixing and the development of a free-jet type gas flow. Gas sampling takes place from the center flow that is fully unaffected by wall interactions. The reaction time was 7.9 s.

Ozone was produced by means of an ozone generator (UVP OG-2). In the case of photolysis experiments, isopropyl nitrite was taken from a gas mixture prepared in a gas-metering unit. Photolysis was carried out downstream the mixing point of the gas streams by means of 8 NARVA 36W Blacklight Blue lamps.

Reactant concentrations were in the range: $[O_3] = (4.6 - 23) \times 10^{11}$, [α-pinene] = $(2.7 - 300) \times 10^{10}$, [isoprene] = $(6.6 - 146) \times 10^{10}$, [isoprene-1-^{13}C] = $(6.6 - 145) \times 10^{10}$ and [ethylene] = $(3.65 - 80.3) \times 10^{11}$ molecules cm^{-3}. Isopropyl nitrite concentrations in the photolysis experiments were $(1.7 - 31) \times 10^{10}$ molecules cm^{-3}.

Detection of RO_2 radicals and accretion products was carried out by means of a CI-APi-TOF (chemical ionization - atmospheric pressure interface - time-of-flight) mass spectrometer (Airmodus, Tofwerk) and a CI3-TOF (chemical ionization time-of-flight) mass spectrometer[29] sampling from the center flow of the free-jet flow system with a rate of 10 L min^{-1} (STP) each. Used reagent ions of the CI-APi-TOF were protonated n-propylamine ($C_3H_7NH_3^+$), acetate (CH_3COO^-) or nitrate (NO_3^-). The CI3-TOF was running in the ammonium mode (NH_4^+). Mass spectra are depicted with the mass-to-charge unit Thompson (Th), where 1 Th = 1 u/e. Given concentrations from CI-APi-TOF measurements are lower end values based on calculated calibration factors. The NH_4^+-CI3-TOF was calibrated using 3-hexanone from a gas standard. More information is given in the Supporting Information (SI).

Results and Discussion

Detection of RO_2 radicals from α-pinene oxidation. First, we focused on the investigation of the formed RO_2 radicals from the combined O_3/OH + α-pinene reaction, which represent the intermediates generating finally the accretion products. Recently, progress has been made for the detection of RO_2 radicals in different reaction systems applying acetate (CH_3COO^-), ammonium (NH_4^+) or protonated n-propylamine ($C_3H_7NH_3^+$) as the reagent ion instead of the mostly used nitrate.[7,20,29] Using these reagent ions, detected main RO_2 radicals from the O_3/OH + α-pinene reaction comprise two groups, i.e. the ozonolysis derived RO_2 radicals O,O-$C_{10}H_{15}(O_2)_xO_2$ with x = 0, 1, 2, 3 and those from the OH radical reaction HO-$C_{10}H_{16}(O_2)_\alpha O_2$ with α = 0, 1, 2 (Figure 1, SI Figure S1).[5-7,18] Bimolecular RO_2 loss processes were unimportant under the chosen reaction conditions because of the relatively low RO_2 radical concentrations mostly far smaller than 10^8 molecules cm^{-3}, the kinetic limitation of bimolecular RO_2 reactions for the reaction time of 7.9 s, and the absence of efficient reaction partners like HO_2 radicals in excess. The detection of the less oxidized RO_2 radicals with x = 0 and α = 0 is reported here for the first time.

Scheme 1 shows the expected pathways leading to the less oxidized RO_2 radicals with x = 0 and α = 0 based on the knowledge given in the literature.[30-33] Ozonolysis of α-pinene leads to two different Criegee intermediates (CI)[34], each of which appear in different conformers[35]. The CIs are formed with excess energy, denoted with an asterisk in the scheme. They can either decompose forming mainly OH radicals and O,O-$C_{10}H_{15}$ alkyl radicals or they are thermalized by collisions with any gas molecule M forming stabilized Criegee intermediates (sCI). Stabilization accounts for about 15% at atmospheric conditions.[36,37] Due to the longer sCI lifetime compared to that of non-thermalized CI, also bimolecular sCI reactions with water vapor or trace gases are possible being competing with the decomposition pathway. The isomeric O,O-$C_{10}H_{15}$ alkyl radicals form the corresponding RO_2 radicals after O_2 addition, O,O-$C_{10}H_{15}(O_2)_xO_2$ with x = 0. OH radicals from the decomposition of Criegee intermediates react readily with α-pinene in the system forming after O_2 addition the isomeric RO_2 radicals HO-$C_{10}H_{16}(O_2)_\alpha O_2$ with α = 0. Subsequently, repetitive RO_2 radical isomerization followed by O_2 addition may take place forming the higher oxidized RO_2 radicals O,O-$C_{10}H_{15}(O_2)_xO_2$ with x = 1, 2, 3 and HO-$C_{10}H_{16}(O_2)_\alpha O_2$ with α = 1, 2. The exact chemical nature of these reaction steps and the chemical structures of the resulting RO_2 radicals are uncertain up to now. In ref.7 the variety of pathways and structures of OH-derived RO_2 radicals from α-pinene oxidation is presented as obtained from theoretical calculations. Here, it will be argued in the following with the chemical formulas only.

The RO_2 radical primarily formed from ozonolysis with x = 0 was consistently detected with high sensitivity by the $C_3H_7NH_3^+$-APi-TOF and the NH_4^+-CI3-TOF while the CH_3COO^--APi-TOF underestimated its concentration by more than three orders of magnitude. Higher oxidized RO_2 radicals with x = 1, 2, 3 were much more efficiently detected by the CH_3COO^--APi-TOF caused by the stronger binding of the $(RO_2)CH_3COO^-$ clusters.[38, 39] The concentrations of the RO_2 radicals with

184 x = 1, 2, 3 were measured in reasonable agreement within a factor of about 2 - 3 applying the three
185 ionization schemes, with exception of the RO_2 radical with x = 3 that was not observed by the NH_4^+-
186 CI3-TOF.
187 In the case of the different RO_2 radicals from the OH + α-pinene reaction, a similar oxidation-state-
188 dependent behavior of the detection sensitivity for the three ionization schemes has been observed as
189 for the ozonolysis derived RO_2 radicals (Figure 1).
190 Furthermore, unambiguous identification of a C_9-RO_2 radical, $C_9H_{15}O_5$, has been achieved by the
191 NH_4^+-CI3-TOF as well as the $C_3H_7NH_3^+$-APi-TOF. The measured $C_9H_{15}O_5$ concentrations, however,
192 did not exceed 4×10^5 molecules cm^{-3} and the importance of $C_9H_{15}O_5$ radicals within the reaction
193 system was assumed to be small.
194 Total ozonolysis products detected by the $C_3H_7NH_3^+$-APi-TOF technique, including RO_2 radicals
195 and the closed-shell products $C_{10}H_{16}O_2$ and $C_{10}H_{16}O_3$, account for 51 - 60 % of the reacted carbon
196 being close to the attainment of the carbon balance (SI Figure S2). Almost identical results have been
197 obtained using protonated ethylamine or n-butylamine as the reagent ion for the aminium-APi-TOF
198 measurements. In the case of the OH radical reaction, however, the total products measured by the
199 $C_3H_7NH_3^+$-APi-TOF account only for 14 - 22 % of the reacted carbon assuming an OH yield of 85 %
200 from α-pinene ozonolysis.[40] The reason for the seemingly low total sensitivity for OH radical products
201 is not clear at the moment and more precise measurements are needed. The carbon balance obtained
202 by the NH_4^+-CI3-TOF measurements is similar to the one of the aminium-APi-TOF due to almost the
203 same sensitivity for the main products.
204

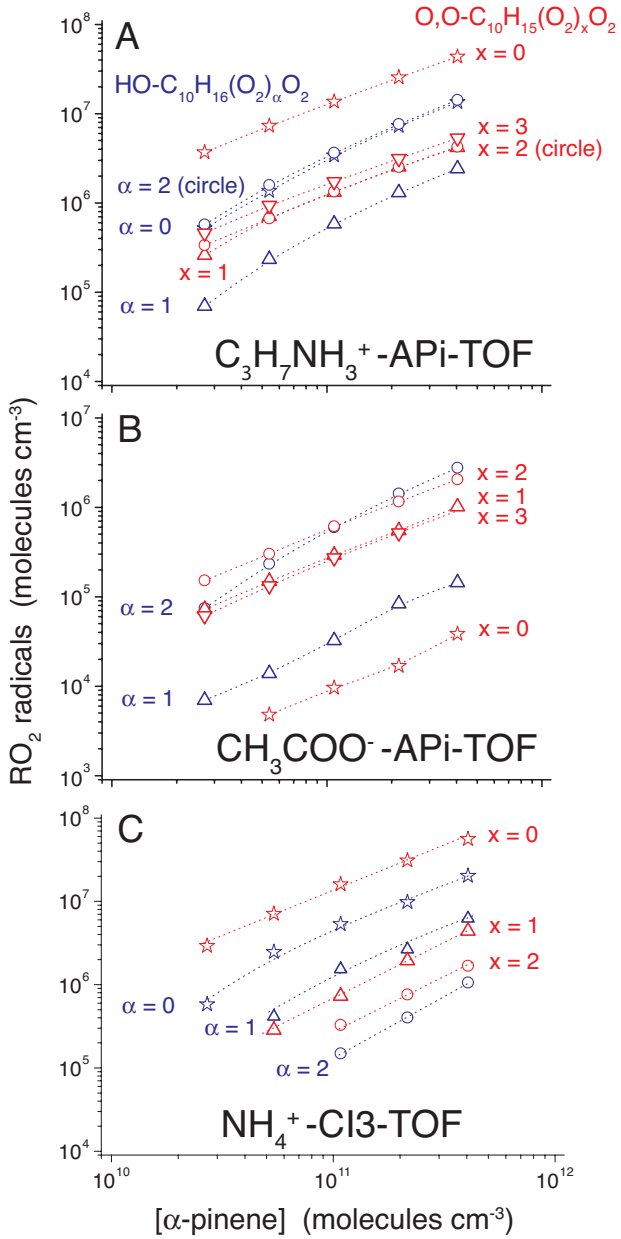

Figure 1. Main RO_2 radicals from the O_3/OH + α-pinene reaction measured by different ionization schemes: **A** $C_3H_7NH_3^+$-APi-TOF, **B** CH_3COO^--APi-TOF, **C** NH_4^+-CI3-TOF. OH radicals were formed by the ozonolysis reaction. Depicted are the ozonolysis derived RO_2 radicals O,O-$C_{10}H_{15}(O_2)_xO_2$ with x = 0, 1, 2, 3 in red and the OH-reaction derived RO_2 radicals HO-$C_{10}H_{16}(O_2)_\alpha O_2$ with α = 0, 1, 2 in blue. Reactant concentrations were $[O_3] = 6.8 \times 10^{11}$ and [α-pinene] = (2.7 - 40.5) × 10^{10} molecules cm^{-3}.

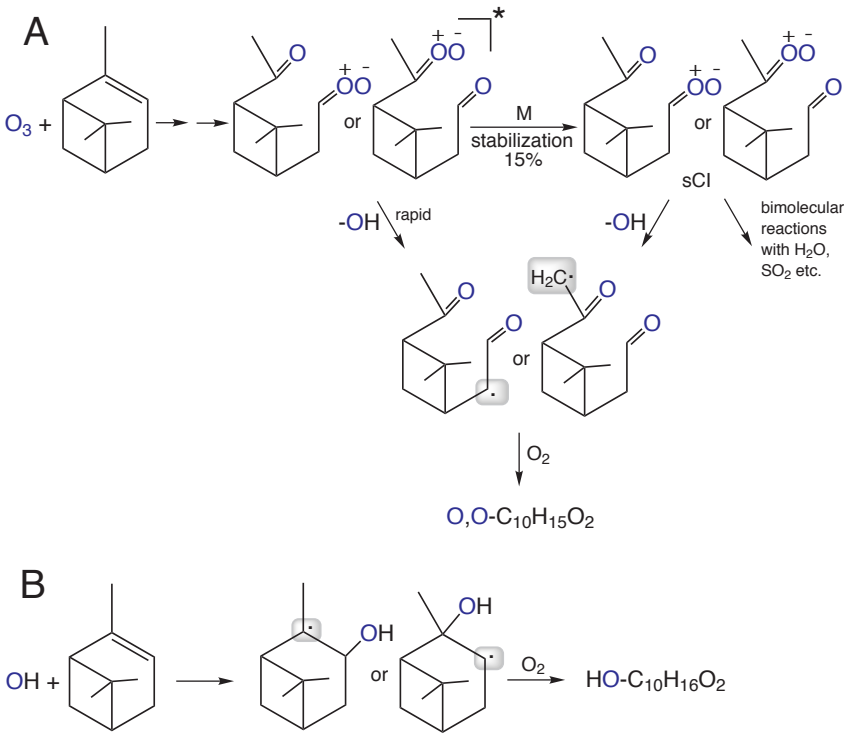

Scheme 1. Reaction scheme for the formation of the first, less oxidized RO_2 radicals **A**: O,O-$C_{10}H_{15}O_2$ from α-pinene ozonolysis and **B**: HO-$C_{10}H_{16}O_2$ from the OH + α-pinene reaction. The asterisk indicates the presence of excess energy, M stands for all gas-phase molecules acting as collision partner. The alkyl radical moiety is highlighted by a shaded oval.

Formation of C_{19}/C_{20} accretion products. Figure 2 shows a mass spectrum from the O_3/OH + α-pinene reaction in the mass range of 380 - 500 Th recorded by the $C_3H_7NH_3^+$-APi-TOF. The spectrum of the extended mass range of 500 - 650 Th is given in SI Figure S3. The measurement in the presence of the OH radical scavenger revealed the accretion products that are exclusively formed via reactions of ozonolysis derived RO_2 radicals, see the upper part in red of Figure 2 and SI Figure S3. Additional experiments on the pure OH + α-pinene reaction, forming OH radicals via photolysis of isopropyl nitrite, disclosed the accretion products that solely arise from OH-reaction derived RO_2 radicals, i.e. $C_{20}H_{34}O_{4,6,8,10,12}$ (SI Figure S4). Their $C_3H_7NH_3^+$-adduct signals are marked in blue in the given spectra (Figure 2, SI Figure S3).

Starting from the 7 main C_{10}-RO_2 radicals generated by the combined O_3/OH + α-pinene reaction (Figure 1), all possible C_{20} accretion products from RO_2 self- and cross-reactions according to pathway (1) have been observed. These are $C_{20}H_{30}O_{6,8,10,12,14,16,18}$ formed solely from ozonolysis derived RO_2 radicals O,O-$C_{10}H_{15}(O_2)_xO_2$ with x = 0, 1, 2, 3, $C_{20}H_{34}O_{4,6,8,10,12}$ from OH-reaction derived RO_2 radicals HO-$C_{10}H_{16}(O_2)_\alpha O_2$ with α = 0, 1, 2 and $C_{20}H_{32}O_{5,7,9,11,13,15}$ from the mixed reactions of both types of RO_2 radicals. The larger number of remaining accretion product signals in the spectra can be explained in a similar way according to pathway (1) but with an involvement of a formal CH_2O elimination. Accordingly, $C_{19}H_{28}O_{5,7,9,11,13}$ can be formed from ozonolysis derived RO_2 radicals and

$C_{19}H_{30}O_{6,8,10,12,14}$ from the mixed reactions of both types of RO_2 radicals. No C_{19} accretion products have been observed as a result of the pure OH + α-pinene reaction. It should be noted, that there is no experimental evidence for a CH_2O release and we cannot state a possible mechanistic explanation for that at the moment. It is just a suggestion that helps to describe the experimental findings. Determination of the exact accretion product masses supports the proposed chemical composition of the accretion products (SI Table S1).

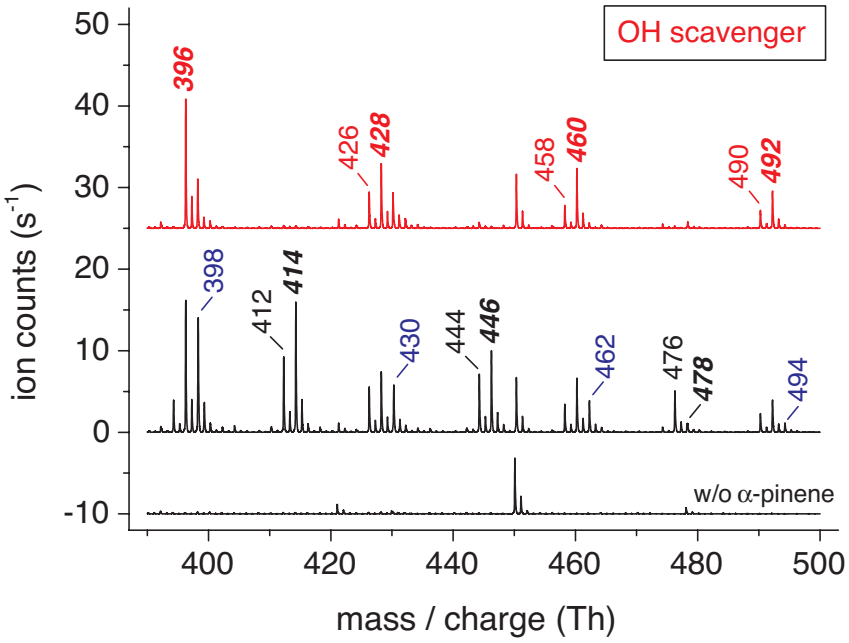

Figure 2. Accretion products from the O_3/OH + α-pinene reaction in the mass range 390 - 500 Th measured by $C_3H_7NH_3^+$-APi-TOF, the upper part in red is obtained in the presence of the OH radical scavenger propane, the lower spectrum "w/o α-pinene" characterizes the background. Reactant concentrations were $[O_3] = 2.3 \times 10^{12}$, [α-pinene] $= 1.2 \times 10^{12}$ and [propane] $= 2.5 \times 10^{16}$ molecules cm^{-3}. Given numbers are nominal masses of the $C_3H_7NH_3^+$-adducts with the accretion products. Color coding of ROOR´ formation via pathway (1):
red: **$C_{20}H_{30}O_{6,8,10}$** via O,O-$C_{10}H_{15}(O_2)_{x1}O_2$ + O,O-$C_{10}H_{15}(O_2)_{x2}O_2$ for $x_1 + x_2 = 0, 1, 2$ (For example: $C_{20}H_{30}O_{10}$ can be formed from RO_2 radicals with $x_1 = 0$ and $x_2 = 2$ or $x_1 = 1$ and $x_2 = 1$, etc.); red italic bold: **$C_{19}H_{28}O_{5,7,9,11}$** via O,O-$C_{10}H_{15}(O_2)_{x1}O_2$ + O,O-$C_{10}H_{15}(O_2)_{x2}O_2$ for $x_1 + x_2 = 0, 1, 2, 3$ incl. CH_2O release; blue: **$C_{20}H_{34}O_{4,6,8,10}$** via HO-$C_{10}H_{16}(O_2)_{\alpha1}O_2$ + HO-$C_{10}H_{16}(O_2)_{\alpha2}O_2$ for $\alpha_1 + \alpha_2 = 0, 1, 2, 3$; black: **$C_{20}H_{32}O_{5,7,9}$** via O,O-$C_{10}H_{15}(O_2)_xO_2$ + HO-$C_{10}H_{16}(O_2)_\alpha O_2$ for $x + \alpha = 0, 1, 2$; black italic bold: **$C_{19}H_{30}O_{6,8,10}$** via O,O-$C_{10}H_{15}(O_2)_xO_2$ + HO-$C_{10}H_{16}(O_2)_\alpha O_2$ for $x + \alpha = 1, 2, 3$ incl. CH_2O release.

We tested for unwanted processes in the ion-molecule reaction (IMR) region of the CI-APi-TOF that could affect the detected signals of the accretion products. To do so, measurements with increased reactant concentrations have been conducted sampling either the undiluted reactions gas or after dilution by a factor of 8.[7,20] The measured accretion product signals decreased by a factor of 6.3 - 8.5

after dilution being in line with the dilution factor within the experimental uncertainty. That confirms that the product formation predominantly takes part in the flow system and not in the IMR region (SI Figure S5).

Accretion product spectra were also recorded applying the mostly used NO_3^--APi-TOF technique[5-7] (SI Figure S6). The spectra are qualitatively in good agreement with the results from the $C_3H_7NH_3^+$-APi-TOF for accretion products with 8 - 9 O atoms or more. For ROOR´ with lower oxygen content, however, the NO_3^--APi-TOF is less sensitive or totally fails to detect them. This behavior is obviously due to missing functional groups in the less oxidized products that prevent sufficient strong binding with the NO_3^- ion.[38,41] Nevertheless, the detectable accretion products by the NO_3^--APi-TOF conclusively support the proposed assignment of ROOR´ products to the reacting RO_2 precursors. Accretion products with 4 or 5 O atoms, not detectable by the NO_3^--APi-TOF, were observed by the NH_4^+-CI3-TOF and the $C_3H_7NH_3^+$-APi-TOF in good agreement including $C_{20}H_{30}O_4$ and $C_{20}H_{30}O_5$ with relatively low concentrations (SI Figure S7). Formation paths leading to $C_{20}H_{30}O_4$ and $C_{20}H_{30}O_5$ are not understood at the moment.

Some studies in the literature point to accretion product formation from ozonolysis experiments based on sCI reactions.[42,43] However, rapid unimolecular decomposition as well as the effective water vapor reactions result in low steady-state sCI concentrations from α-pinene ozonolysis[44] making an efficient sCI contribution to the accretion product formation questionable, at least for close to atmospheric reactant conditions. We tested for possible sCI reactions forming accretion products by adding acetic acid as sCI scavenger. Acetic acid additive of 5.0×10^{12} molecules cm^{-3} results in an additional sCI loss rate of 10^3 s^{-1} assuming a CH_3COOH + sCI rate coefficient of 2×10^{-10} cm^3 $molecule^{-1}$ s^{-1}.[45] The addition of acetic acid yielded a measureable lowering of the RO_2 radical concentrations in the range of 11 - 17% due to suppression of the unimolecular sCI decomposition, that forms the precursors of the RO_2 radicals O,O-$C_{10}H_{15}(O_2)_xO_2$ and HO-$C_{10}H_{16}(O_2)_\alpha O_2$ to some extent, see Scheme 1. It is to be noted, that a new, very strong signal appeared, which is consistent with an addition product of CH_3COOH + sCI. The comparison of the accretion product spectrum in the presence of acetic acid, upper part, with that in absence of the addition is depicted in Figure 3. In the whole spectrum, accretion product signals from the sCI scavenger experiment were about 20 - 30% lower compared to the basis spectrum. This behavior reflects the square dependence of RO_2 concentrations for the ROOR´ formation kinetics according to pathway (1). Reduction of RO_2 concentrations by 11 - 17% should theoretical lead to a lowering of the ROOR´ concentrations by 21 - 31%. Thus, as a result of the sCI scavenger experiments there were no indications for sCI-driven accretion product formation. The finding is supported by the outcome of the pure OH + α-pinene reaction in total absence of Criegee intermediates, that also gave rise to the five possible ROOR´ products, $C_{20}H_{34}O_{4,6,8,10,12}$, from HO-$C_{10}H_{16}(O_2)_\alpha O_2$ with $\alpha = 0, 1, 2$ (SI Figure S4).

Moreover, also any heterogeneous process for accretion product formation[46] is highly unlikely because wall interactions are strongly suppressed in the used flow system.

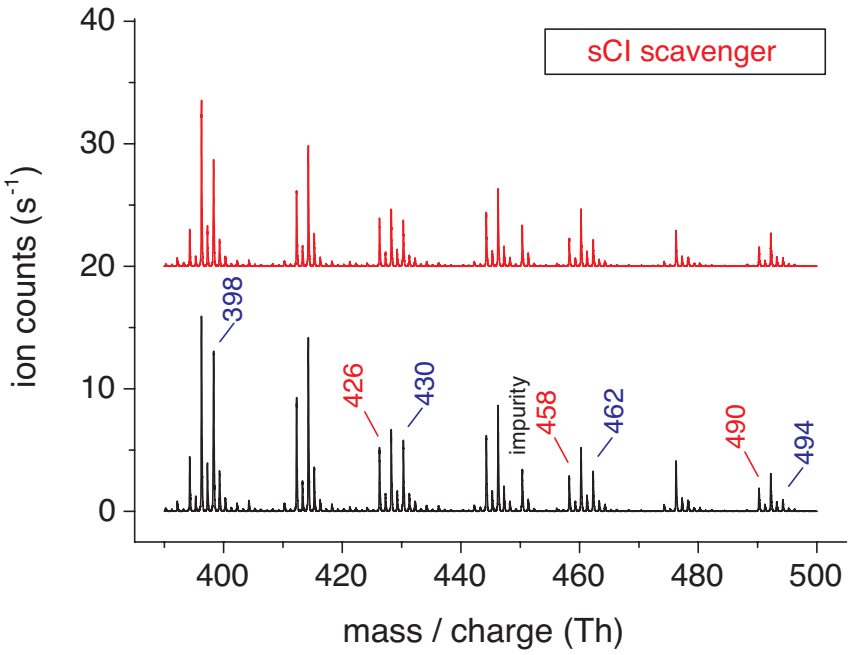

Figure 3. Accretion products from the O_3/OH + α-pinene reaction in the mass range 390 - 500 Th measured by $C_3H_7NH_3^+$-APi-TOF, the upper part in red is obtained in the presence of the sCI scavenger. Reactant concentrations were $[O_3] = 2.3 \times 10^{12}$, [α-pinene] = 1.2×10^{12} and [acetic acid] = 5.0×10^{12} molecules cm^{-3}. Stated nominal masses of the $C_3H_7NH_3^+$-adducts with ROOR´ belong to $C_{20}H_{30}O_{6,8,10}$ (in red) formed from ozonolysis derived RO_2 radicals and $C_{20}H_{34}O_{4,6,8,10}$ (in blue) from OH-reaction derived RO_2 radicals.

Kinetics of accretion product formation. The free-jet flow system allows conducting the experiments with negligible wall interactions. Particles were not present in the purified feed gas and new particle formation did not take place due to the low reactant conversion and the short reaction time. Thus, RO_2 radical and accretion product concentrations were not influenced by unwanted wall losses or gas/particle partitioning, which admits the determination of rate coefficients based on measured reactant and product concentrations. The C_{19}/C_{20} product concentrations, ROOR´, showed a square dependence regarding increasing α-pinene concentrations for constant O_3 (Figure 4), i.e. a slope of about 2 for log([ROOR´]) vs. log([α-pinene]), that also stands for a square dependence with respect to reacted α-pinene. The RO_2 radicals increased almost linearly with rising α-pinene conversion (Figure 1, SI Figure S8). This behavior is in line with the 2nd order kinetics of accretion product formation according to pathway (1) starting from the respective RO_2 radicals.

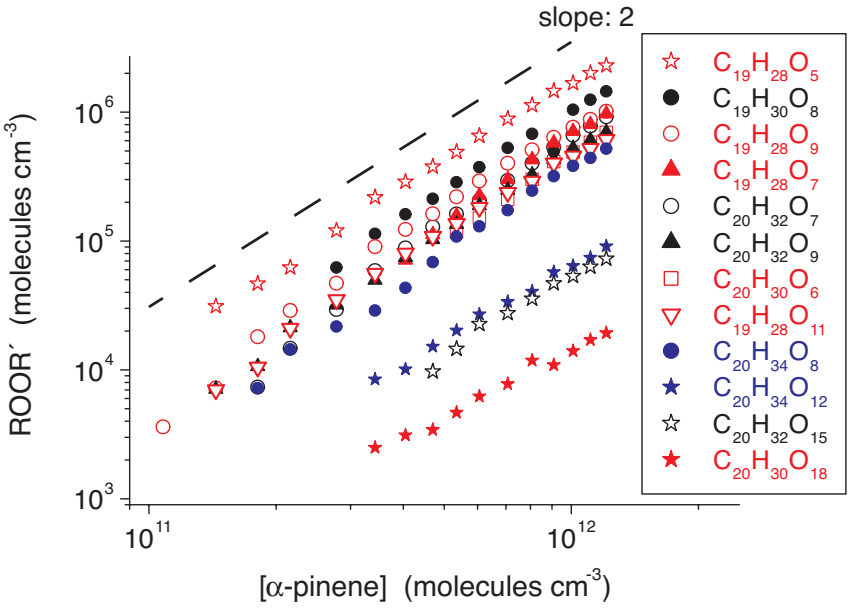

Figure 4. A series of C_{19}/C_{20} accretion products, ROOR´, from the O_3/OH + α-pinene reaction as a function of the α-pinene concentration for constant O_3 measured by $C_3H_7NH_3^+$-APi-TOF. The dashed line represents the slope of 2 for log([ROOR´]) vs. log([α-pinene]). Reactant concentrations were $[O_3] = 6.4 \times 10^{11}$ and [α-pinene] = (1.08 - 12.1) × 10^{11} molecules cm^{-3}. The respective measurements of RO_2 radicals are given in SI Figure S8.

For the chosen experimental conditions, RO_2 radical concentrations increased linearly with time and RO_2 consuming reaction steps did not significantly influence their concentrations (SI Figure S9). Hence, the rate coefficients k_1 of accretion product formation via pathway (1) can be estimated in a simple manner according to equation (I) using the measured concentrations of ROOR´ and RO_2 radicals at the reaction time t, see Supporting Information (SI):

$$k_1 = \frac{[ROOR']_t}{[RO_2]_t \; x \; [R'O_2]_t} \; \frac{3}{t} \qquad (I)$$

It is assumed that the highest oxidized RO_2 radicals, O,O-$C_{10}H_{15}(O_2)_xO_2$ with x = 3 and HO-$C_{10}H_{16}(O_2)_\alpha O_2$ with α = 2 are detected with close to maximum sensitivity by the $C_3H_7NH_3^+$-APi-TOF due to the expected high content of oxygen-containing moieties and the strong binding with the reagent ion. High sensitivity detection can also be assumed for O,O-$C_{10}H_{15}O_2$, the predominant RO_2 radical from ozonolysis, because of the carbon balance of ozonolysis products of up to 60%. That justifies selection of their reactions for the estimation of rate coefficients of ROOR´ formation. Accretion products according to pathway (1), which can be attributed to reactions of the chosen RO_2 radicals with reasonable certainty, are $C_{20}H_{30}O_{18}$, $C_{20}H_{34}O_{12}$ and $C_{20}H_{30}O_6$ from the respective self-reactions and $C_{20}H_{32}O_{15}$ from the cross-reaction of O,O-$C_{10}H_{15}(O_2)_3O_2$ with HO-$C_{10}H_{16}(O_2)_2O_2$. The

kinetic analysis based on equation (I) revealed the expected linear dependence $[ROOR´]_t$ vs. $[RO_2]_t \times [R´O_2]_t$ properly (SI Figure S10). The corresponding rate coefficients are in the range (9.7 - 79) $\times 10^{-12}$ cm^3 $molecule^{-1}$ s^{-1} with an assumed uncertainty being not higher than a factor of 3 (Table 1). Additionally, rate coefficients of the RO_2 self-reactions with respect to ROOR´ formation of $C_6H_{13}O_2$, HO-$C_5H_8O_2$ and HO-$C_9H_{12}(O_2)O_2$ from the OH radical reaction with n-hexane, isoprene and mesitylene (1,3,5-trimethylbenzene), respectively, are shown in Table 1 for comparison. [20] The rate coefficients cover a range of more than three orders of magnitude. The RO_2 reactivity in the process of accretion product formation increases with rising functionalization of the RO_2 radicals[20] and probably with the RO_2 size as well. Comprehensive experimental studies, including theoretical investigations, are needed to get a deeper insight into the ROOR´ formation process on molecular level.

Table 1. Selected rate coefficients of accretion product formation via $RO_2 + R´O_2 \rightarrow ROOR´ + O_2$ from the O_3/OH + α-pinene reaction and comparison with data from a former study[20]. T = 297 ± 1 K

RO_2	$R´O_2$	k (cm^3 $molecule^{-1}$ s^{-1})
O,O-$C_{10}H_{15}O_2$	O,O-$C_{10}H_{15}O_2$	9.7×10^{-12}
HO-$C_{10}H_{16}(O_2)_2O_2$	HO-$C_{10}H_{16}(O_2)_2O_2$	3.7×10^{-11}
O,O-$C_{10}H_{15}(O_2)_3O_2$	O,O-$C_{10}H_{15}(O_2)_3O_2$	4.8×10^{-11}
HO-$C_{10}H_{16}(O_2)_2O_2$	O,O-$C_{10}H_{15}(O_2)_3O_2$	7.9×10^{-11}
[a] HO-$C_5H_8O_2$	O,O-$C_{10}H_{15}(O_2)_xO_2$ x = 0 - 3	(1.3 - 2.3) $\times 10^{-11}$
[b] HO-$C_2H_4O_2$	O,O-$C_{10}H_{15}(O_2)_xO_2$ x = 0 - 3	(1.2 - 3.6) $\times 10^{-11}$
[c] $C_6H_{13}O_2$ (from OH + n-hexane)	$C_6H_{13}O_2$	9.2×10^{-14}
[c] HO-$C_5H_8O_2$ (from OH + isoprene)	HO-$C_5H_8O_2$	6.0×10^{-13}
[c] HO-$C_9H_{12}(O_2)O_2$ (from OH + mesitylene)	HO-$C_9H_{12}(O_2)O_2$	(1.4 - 2.5) $\times 10^{-10}$ [d]

[a] from experiments with isoprene addition
[b] from experiments with ethylene addition
[c] ref.20
[d] results from different reaction conditions

Addition of isoprene or ethylene. Experiments in the presence of isoprene, C_5H_8, or ethylene, C_2H_4, demonstrate how additional RO_2 radicals, i.e. HO-$C_5H_8O_2$ or HO-$C_2H_4O_2$, modify the accretion product formation in the O_3/OH + α-pinene system.

Figure 5 shows the measured RO_2 radical concentrations from a series with rising isoprene addition and otherwise constant reaction conditions. Increasing isoprene concentrations led to lowering of the steady-state OH radical concentration due to enhanced OH consumption by the OH + isoprene reaction, see calculated OH radical concentration "OH calc.". Accordingly, concentrations of OH-reaction derived RO_2 radicals, HO-$C_{10}H_{16}(O_2)_\alpha O_2$ with α = 1, 2 shown in Figure 5, decreased while HO-$C_5H_8O_2$ radical concentrations grew up nearing a maximum level for [isoprene] / [α-pinene] > 3 with more than 85% OH consumption by isoprene, k(OH+isoprene, 298 K) = 1.0×10^{-10} and k(OH+α-pinene, 298 K) = 5.3×10^{-11} cm^3 $molecule^{-1}$ s^{-1}.[47] The measured HO-$C_5H_8O_2$ concentrations were within a factor of 2 of the calculated values. Moreover, a signal appeared at the nominal product mass of 101 Th that was attributed to the RO_2 radical $C_4H_5(O)O_2$ formed most likely from the C_4 Criegee intermediate of isoprene ozonolysis.[48] Within the present study, no effort was undertaken for the identification of products of $C_4H_5(O)O_2$ due to its low concentration and the expected small importance for product formation. The formation and the resulting concentrations of ozonolysis derived RO_2 radicals, O,O-$C_{10}H_{15}(O_2)_xO_2$ with x = 0 and 2 given in Figure 5, were not influenced by the isoprene addition due to the unchanged ozone concentration and the small importance of RO_2 radical consuming reactions for the RO_2 radical concentrations.

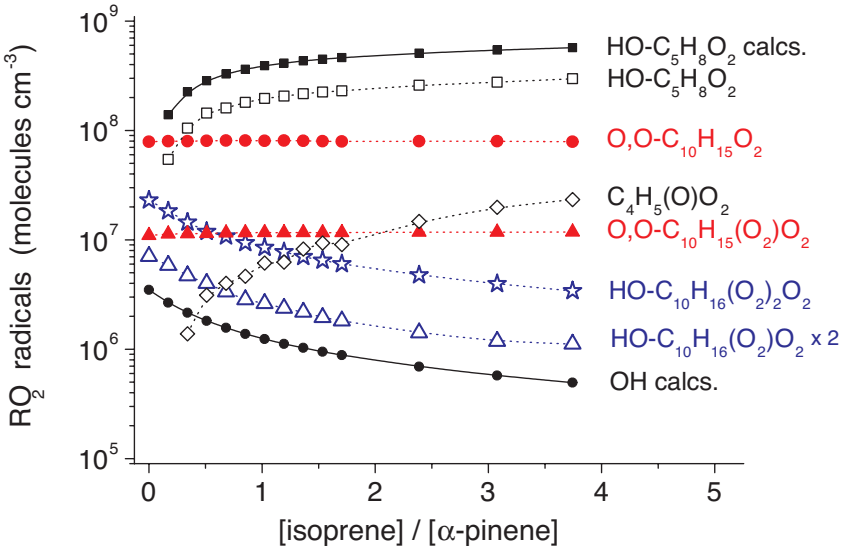

Figure 5. RO_2 radicals from the O_3/OH + α-pinene reaction for increasing isoprene addition and otherwise constant reactant conditions. HO-$C_5H_8O_2$ and $C_4H_5(O)O_2$ formed from isoprene have been measured by the NH_4^+-CI3-TOF, the C_{10}-RO_2 radicals by the $C_3H_7NH_3^+$-APi-TOF. Concentrations of ozonolysis derived RO_2 radicals are depicted in red and the OH-reaction derived RO_2 radicals in blue. "HO-$C_5H_8O_2$ calcs." and "OH calcs." were obtained by modeling. Reactant concentrations were $[O_3] = 2.0 \times 10^{12}$, [α-pinene] = 3.9×10^{11} and [isoprene] = (0 - 1.46) × 10^{12} molecules cm^{-3}.

Concentrations of the accretion products strictly followed the behavior of their RO_2 radical precursors with rising isoprene addition according to the kinetics of the respective RO_2 self- and cross-reactions via pathway (1) (Figure 6). Hence, accretion products ROOR´ arising solely from ozonolysis derived RO_2 radicals were unaffected by the isoprene additives due to the unaffected concentrations of ozonolysis derived RO_2 radicals, e.g. $C_{19}H_{28}O_7$ and $C_{19}H_{28}O_{11}$ in Figure 6A. Concentrations of ROOR´ formed from cross-reactions of OH-reaction derived and ozonolysis derived RO_2 radicals dropped down in parallel to the declining OH level in the experiment, see $C_{19}H_{30}O_8$ and $C_{20}H_{32}O_9$ in Figure 6A. A steeper decrease than the declining OH level was detected for ROOR´ that are formed from two OH-reaction derived RO_2 radicals, again in line with the expected behavior, see $C_{20}H_{34}O_8$ in Figure 6A. Generally, the experiments with additional RO_2 radicals, here shown for HO-$C_5H_8O_2$ radicals, confirmed the attribution of the reacting C_{10}-RO_2 radicals to the observed C_{19}/C_{20} accretion products as described before.

With increasing isoprene addition, rising signals of C_{15} accretion products from the reaction of HO-$C_5H_8O_2$ radicals with C_{10}-RO_2 radicals emerged in the spectrum. Figure 6B shows the occurrence of the 4 possible ROOR´ products, $C_{15}H_{24}O_{5,7,9,11}$, from the reaction of HO-$C_5H_8O_2$ radicals with O,O-$C_{10}H_{15}(O_2)_xO_2$ radicals with x = 0, 1, 2, 3. Experiments with isoprene-1-^{13}C confirmed the signal assignment. Kinetic analysis of the accretion product formation according to pathway (1) led to rate coefficients in the range of (1.3 - 2.3) × 10^{-11} cm^3 $molecule^{-1}$ s^{-1} for the C_{15} products (Table 1, SI Figure S11). It should be noted that also the signal of $C_{10}H_{18}O_4$ from the HO-$C_5H_8O_2$ radical self-reaction via pathway (1) was detected in line with the finding of a former study.[20]

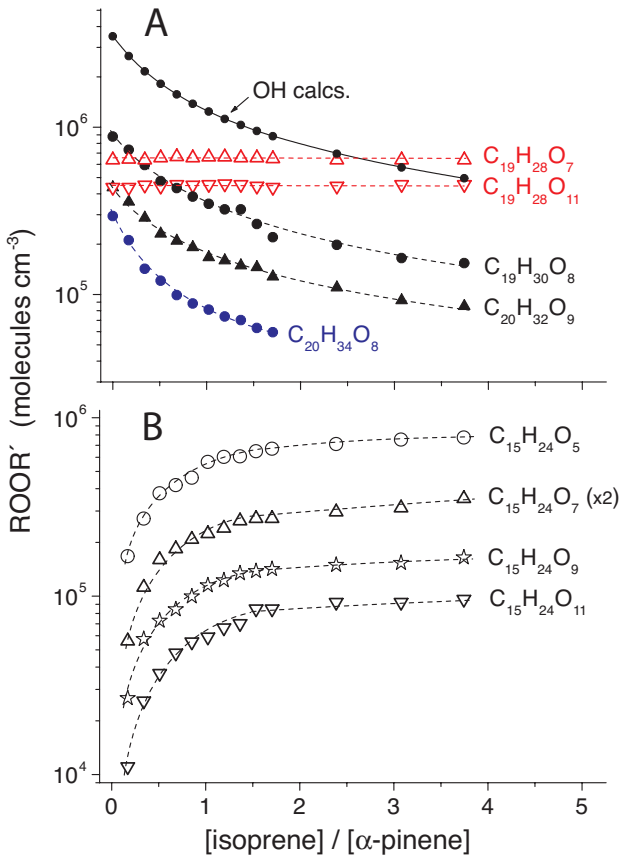

Figure 6. Accretion product formation from the O_3/OH + α-pinene reaction as a function of increasing isoprene addition. **A:** C_{19}/C_{20} products solely formed from ozonolysis derived RO_2 radicals in red, solely from OH-reaction derived RO_2 radicals in blue and those from both types of RO_2 radicals in black. **B:** C_{15} products from the reaction of HO-$C_5H_8O_2$ radicals with O,O-$C_{10}H_{15}(O_2)_xO_2$ radicals with x = 0, 1, 2, 3. All products have been measured by the $C_3H_7NH_3^+$-APi-TOF. Reaction conditions are stated in the caption of Figure 5.

Experiments with ethylene addition revealed the same behavior for the C_{10}-RO_2 radicals and C_{19}/C_{20} accretion products as observed in the case of runs with isoprene addition. Due to its lower OH reactivity, ethylene was applied in a larger excess over α-pinene than isoprene, k(OH+ethylene, 298 K) = 8.5×10^{-12} cm^3 molecule^{-1} s^{-1}.[47] Cross-reactions of HO-$C_2H_4O_2$ radicals with C_{10}-RO_2 radicals formed the corresponding C_{12} accretion products. SI Figure S12 shows the concentrations of $C_{12}H_{20}O_{5,7,9,11}$ from the reaction with O,O-$C_{10}H_{15}(O_2)_xO_2$ radicals with x = 0, 1, 2, 3. The corresponding rate coefficients were in the range of $(1.2 - 3.6) \times 10^{-11}$ cm^3 molecule^{-1} s^{-1} (Table 1, SI Figure S13).

Moreover, also the OH radical scavenger experiments with propane have been analyzed with respect to new accretion product formation. Presence of high propane concentrations leads to the formation of propyl peroxy radicals, $C_3H_7O_2$, instead of HO-$C_{10}H_{16}(O_2)_\alpha O_2$ radicals. The $C_3H_7O_2$ radicals formed C_{13} accretion products from the reaction with ozonolysis derived C_{10}-RO_2 radicals O,O-$C_{10}H_{15}(O_2)_xO_2$ according to pathway (1) (SI Figure S14). This finding further supports the

universal validity of accretion product formation from all RO_2 radical combinations in a reaction system.

Atmospheric implications. The measurements showed that C_{20} accretion products according to pathway (1) have been formed from all possible combinations of the 7 main C_{10}-RO_2 radicals. Additionally, C_{19} accretion products occurred whose formation can be tentatively explained in an analogous way assuming CH_2O elimination. With that, almost the whole accretion product distribution can be mechanistically explained. Obtained rate coefficients of RO_2 radical self- and cross-reaction according to pathway (1) are in the range $(9.7 - 79) \times 10^{-12}$ cm^3 $molecule^{-1}$ s^{-1} being similar or slightly higher than the k-values of $(5 - 20) \times 10^{-12}$ cm^3 $molecule^{-1}$ s^{-1} generally applied for the major RO_2 loss reactions with NO or HO_2 radicals.[11-13] The relatively high rate coefficients of C_{10}-RO_2 radical cross-reactions with HO-$C_5H_8O_2$ or HO-$C_2H_4O_2$ (Table 1) suggest that effective accretion product formation is possible with a number of other RO_2 radicals present in the atmospheric reaction system, such as those generated from other alkenes or aromatics.[23-25] Thus, a complex accretion product spectrum can be expected as already proposed from an experimental study with a series of model RO_2 radicals.[20] A reasoned evaluation of the role of RO_2 radical self- and cross-reaction according to pathway (1) for different situations in the atmosphere is possible based on the rate coefficients obtained in this study and from the former study[20].

In atmospheric science the mechanistic explanation of early particle growth suppression in isoprene-dominated forestlands[27,49] is still an open question. In a recent field study carried out in a mixed deciduous forest in Alabama, no growth of sub-2 nm particles was observed while C_9 and C_{10} low-volatility oxygenated products (HOMs) from α-pinene oxidation were measured with mixing ratios of 20 - 30 pptv.[27] This behavior stands in stark contrast to the expected growth rates by HOMs from pure α-pinene oxidation as deduced from a chamber study.[26] Moreover, suppression of particle formation by isoprene was reported as a result of a plant chamber experiment, which was simply explained by lowering of the OH radical level in the system due to the isoprene additive.[50] In the atmosphere, however, the OH radical concentration is not lowered in isoprene-dominated areas calling a direct application of the plant chamber findings to the atmosphere into question.[51]

We suppose that probably the C_{19}/C_{20} accretion products play a critical role for the early particle growth, rather than the C_9/C_{10} HOMs, and performed modeling calculations for atmospheric daytime conditions with different isoprene / α-pinene ratios. The modeling considered constant oxidant concentrations of OH radicals and ozone of 2×10^6 and 7.5×10^{11} molecules cm^{-3}, respectively, and constant concentrations of HO_2 radicals and NO that are defining the main loss reactions of the RO_2 radicals. Rate coefficients for accretion product formation were taken from the present study, see Supporting Information (SI). 2-fold isoprene excess over α-pinene, representing the Alabama conditions, led to a reduction of the C_{10}-RO_2 radical concentration of about 10% and in the case of a

15-fold isoprene excess, as present in the Amazon forest, to a reduction of 48% (SI Figure S15).[23,27] Consequently, the concentrations of the C_{19}/C_{20} accretion products dropped down by a factor of 1.2 and 3.6, respectively. Concentrations of the C_{15} products substantially increased with rising isoprene excess. As a result of the modeling, it is difficult to assume that C_{19}/C_{20} product reduction of only ~20 % for the Alabama case can explain early growth suppression by isoprene. Further studies are needed in order to discover reasons for early growth suppression in isoprene-dominated forestlands, such as in Alabama or in the Amazon forest.

Associated Content

Supporting Information

The Supporting Information is available free of charge on the ACS Publication website at …

Additional Information regarding instrumental analysis, kinetic analysis and other materials are shown in Figures S1 - S15 and Table S1.

Notes

The authors declare no competing financial interest.

Acknowledgements

We thank K. Pielok and A. Rohmer for technical assistance, the tofTools team for providing a data analysis toolbox, the Austrian Research Funding Association (FFG. Project Number 846050) for financial support and IONICON Analytik GmbH for in-kind contributions within the funded project.

References

(1) Sindelarova, K.; Grainer, C.; Bouarar, I.; Guenther, A.; Tilmes, S.; Stavrakou, T.; Müller, J.-F.; Kuhn, U.; Stefani, P.; Knorr, W. Global data set of biogenic VOC emissions calculated by the MEGAN model over the last 30 years. *Atmos. Chem. Phys.* **2014**, *14*, 9317-9341.

(2) Goldstein, A.H.; Galbally, I.E. Known and unexplored organic constituents in the Earth´s atmosphere. *Environ. Sci. Technol.* **2007**, *41*, 1514-1521.

(3) Seinfeld, J.H.; Pandis, S.N. Atmospheric Chemistry and Physics: From Air Pollution to Climate Change (Wiley, New York, 1998).

(4) Crounse, J.D.; Nielsen, L.B.; Jørgensen, S.; Kjaergaard, H.G.; Wennberg, P.O. Autoxidation of organic compounds in the atmosphere. *J. Phys. Chem. Lett.* **2013**, *4*, 3513-3520.

(5) Ehn, M.; Thornton, J. A.; Kleist, E.; Sipilä, M.; Junninen, H.; Pullinen, I.; Springer, M.; Rubach, F.; Tillmann, R.; Lee, B.; Lopez-Hilfiker, F.; Andres, S.; Acir, I. H.; Rissanen, M.; Jokinen, T.; Schobesberger, S.; Kangasluoma, J.; Kontkanen, K.; Nieminen, T.; Kurtén, T.; Nielsen, L. B.; Jørgensen, S.; Kjaergaard, H. K.; Canagaratna, M.; Maso, M. D.; Berndt, T.; Petäjä, T.; Wahner, A.; Kerminen, V.-M.; Kulmala, M.; Worsnop, D. R.; Wildt, J.; Mentel, T. F. A large source of low-volatility secondary organic aerosol. *Nature* **2014**, *506*, 476-479.

(6) Jokinen, T.; Sipilä, M.; Richters, S.; Kerminen, V. M.; Paasonen, P.; Stratmann, F.; Worsnop, D.; Kulmala, M.; Ehn, M.; Herrmann, H.; Berndt, T. Rapid autoxidation forms highly oxidized RO_2 radicals in the atmosphere. *Angew. Chem. Int. Ed.* **2014**, 53, 14596-14600.

(7) Berndt, T.; Richters, S.; Jokinen, T.; Hyttinen, N.; Kurtén, T.; Otkjær, R. V.; Kjaergaard, H. K.; Stratmann, F.; Herrmann, H.; Sipilä, M.; Kulmala, M.; Ehn, M. Hydroxyl radical-induced formation of highly oxidized organic compounds. *Nat. Commun.* **2016**, *7*, 13677.

(8) Praske, E.; Otkjaer, R.V.; Crounse, J.D.; Hethrox, J.C.; Stoltz, B.M.; Kjaergaard, H.G.; Wennberg, P.O. Atmospheric autoxidation is increasingly important in urban and suburban North America. *Proc. Natl. Acad. Sci. USA* **2018**, *115*, 64-69.

(9) Vereecken, L.; Müller, J.-F.; Peeters, J. Low-volatility poly-oxygenates in the OH-initiated atmospheric oxidation of α-pinene: impact of non-traditional peroxyl radical chemistry. *Phys. Chem. Chem. Phys.* **2007**, *9*, 5241-5248.

(10) Richters, S.; Pfeifle, M.; Olzmann, M.; Berndt, T. *endo*-Cyclization of unsaturated RO_2 radicals from the gas-phase ozonolysis of cyclohexadienes. *Chem. Commun.* **2017**, *53*, 4132-4135.

(11) Lightfoot, P.D.; Cox, R.A.; Crowley, J.N.; Destriau, M.; Hayman, G.D.; Jenkin, M.E.; Moortgat, G.K.; Zabel, F. Organic peroxy radicals: Kinetics, spectroscopy and tropospheric chemistry. *Atmos. Environ.* **1992**, 26, 1805-1961.

(12) Wallington, T.J.; Dagaut, P.; Kurylo, M.J. UV absorption cross sections and reaction kinetics and mechanisms for peroxy radicals in the gas phase. *Chem. Rev.* **1992**, *92*, 667-710.

(13) Orlando, J.J.; Tyndall, G.S. Laboratory studies of organic peroxy radical chemistry: an overview with emphasis on recent issues of atmospheric significance. *Chem. Soc. Rev.* **2012,** *41*, 6294-6317.

(14) Weaver, J.; Meagher, J.; Shortridge, R.; Heicklen, J. The oxidation of acetyl radicals. *J. Photochem.* **1975**, *4*, 341-360.

(15) Anastasi, C.; Waddington, D.J.; Woolley, A. Reactions of oxygenated radicals in the gas phase. *J. Chem. Soc., Faraday Trans. 1* **1983**, *79*, 505-516.

(16) Mentel, T. F.; Springer, M.; Ehn, M.; Kleist, E.; Pullinen, I.; Kurtén, T.; Rissanen, M. P.; Wahner, A.; Wildt, J. Formation of highly oxidized multifunctional compounds: Autoxidation of peroxy radicals formed in the ozonolysis of alkenes-deduced from structure–product relationships. *Atmos. Chem. Phys.* **2015**, *15*, 6745-6765.

(17) Berndt, T.; Richters, S.; Kaethner, R.; Voigtländer, J.; Stratmann, F.; Sipilä, M.; Kulmala, M.; Herrmann, H. Gas-phase ozonolysis of cycloalkenes: Formation of highly oxidized RO_2 radicals and their reactions with NO, NO_2, SO_2, and other RO_2 radicals. *J. Phys. Chem. A* **2015**, *119*, 10336-10348.

(18) Jokinen, T.; Berndt, T.; Makkonen, R.; Kerminen, V.-M.; Junninen, H.; Paasonen, P.; Stratmann, F.; Herrmann, H.; Guenther, A.; Worsnop, D. R.; Kulmala, M.; Ehn, M.; Sipilä, M. Production of extremely low volatile organic compounds from biogenic emissions: Measured yields and atmospheric implications. *Proc. Natl. Acad. Sci. USA* **2015**, *112*, 7123-7128.

(19) Zhang, X.; Lambe, A. T.; Upshur, M. A.; Brooks, W. A.; Be, A. G.; Thomson, R. J.; Geiger, F. M.; Surrat, J. D.; Zhang, Z.; Gold, A.; Graf, S.; Cubison, M. J.; Groessl, M.; Jayne, J. T.; Worsnop, D. R.; Canagaratna, M. R. Highly oxygenated multifunctional compounds in α-pinene secondary organic aerosol. *Environ. Sci. Technol.* **2017**, *51*, 5932-5940.

(20) Berndt, T.; Scholz, W.; Mentler, B.; Fischer, L.; Herrmann, H.; Kulmala, M.; Hansel, A. Accretion product formation from self- and cross-reactions of RO_2 radicals in the atmosphere. *Angew. Chem. Int. Ed.* **2018**, *57*, 3820-3824.

(21) Kulmala, M.; Kontkanen, J.; Junninen, H.; Lehtipalo, K.; Manninen, H. E.; Nieminen, T.; Petäjä, T.; Sipilä, M.; Schobesberger, S.; Rantala, P.; Franchin, A.; Jokinen, T.; Järvinen, E.; Äijälä, M.; Kangasluoma, J.; Hakala, J.; Aalto, P. P.; Paasonen, P.; Mikkilä, J.; Vanhanen, J.; Aalto, J.; Hakola, H.; Makkonen, U.; Ruuskanen, T.; Mauldin III, R. L.; Duplissy, J.; Vehkamäki, H.; Bäck, J.; Kortelainen, A.; Riipinen, I.; Kurtén, T.; Johnston, M. V.; Smith, J. N.; Ehn, M.; Mentel, T. F.; Lehtinen, K. E. J.; Laaksonen, A.; Kerminen, V.-M.; Worsnop, D. R. Direct observation of atmospheric aerosol nucleation. *Science* **2013**, *339*, 943-946.

(22) Mohr, C.; Lopez-Hilfiker, F. D.; Yli-Juuti, T.; Heitto, A.; Lutz, A.; Hallquist, M.; D´Ambro, E. L.; Rissanen, M. P.; Hao, L.; Schobesberger, S.; Kulmala, M.; Mauldin III, R. L.; Makkonen, U.; Sipilä, M.; Petäjä, T.; Thornton, J. A. Ambient observation of dimers from

terpene oxidation in the gas phase: Implications for new particle formation and growth. *Geophys. Res. Lett.* **2017**, *44*, 2958-2966.

(23) Zimmerman, P.R.; Greenberg, J.P.; Westberg, C.E. Measurements of atmospheric hydrocarbons and biogenic emission fluxes in the Amazon boundary layer. *J. Geophys. Res.* **1988**, *93*, 1407-1416.

(24) Hakola, H.; Laurila, T.; Rinne, J.; Puhto, K. The ambient concentrations of biogenic hydrocarbons at a northern European, boreal site. *Atmos. Environ.* **2000**, *34*, 4971-4982.

(25) Fehsenfeld, F.; Calvert, C.; Fall, R.; Goldan, P.; Guenther, A. B.; Hewitt, C. N.; Lamb, B.; Liu, S.; Trainer, M.; Westberg, H.; Zimmermann, P. Emissions of volatile organic compounds from vegetation and the implications for atmospheric chemistry. *Global Biogeochemical Cycles* **1992**, *6*, 389-430.

(26) Tröstl, J.; Chuang, W. K.; Gordon, H.; Heinritzi, M.; Yan, C.; Molteni, U.; Ahlm, L.; Frege, C.; Bianchi, F.; Wagner, R.; Simon, M.; Lehtipalo, K.; Williamson, C.; Craven, J. S.; Duplissy, J.; Adamov, A.; Almeida, J.; Bernhammer, A.-K.; Breitenlechner, M.; Brilke, S.; Dias, A.; Ehrhart, S.; Flagan, R. C.; Franchin, A.; Fuchs, C.; Guida, R.; Gysel, M.; Hansel, A.; Hoyle, C. R.; Jokinen, T.; Junninen, H.; Kangasluoma, J.; Keskinen, H.; Kim, J.; Krapf, M.; Kürten, A.; Laaksonen, A.; Lawler, M.; Leiminger, M.; Mathot, S.; Möhler, O.; Nieminen, T.; Onnela, A.; Petäjä, T.; Piel, F. M.; Miettinen, P.; Rissanen, M. P.; Rondo, L.; Sarnela, N.; Schobesberger, S.; Sengupta, K.; Sipilä, M.; Smith, J. N.; Steiner, G.; Tomè, A.; Virtanen, A.; Wagner, A. C.; Weingartner, E.; Wimmer, D.; Winkler, P. M.; Ye, P.; Carslaw, K. S.; Curtius, J.; Dommen, J.; Kirkby, J.; Kulmala, M.; Riipinen, I.; Worsnop, D. R.; Donahue, N. M.; Baltensperger, U. The role of low-volatility organic compounds in initial particle growth in the atmosphere. *Nature* **2016**, *533*, 527-531.

(27) Lee, S.-H.; Uin, J.; Guenther, A. B.; de Gouw, J. A.; Yu, F.; Nadykto, A. B.; Herb, J.; Ng, N. L.; Koss, A.; Brune, W. H.; Baumann, K.; Kanawade, V. P.; Keutsch, F. N.; Nenes, A.; Olsen, K.; Goldstein, A.; Ouyang, Q. Isoprene suppression of new particle formation: Potential mechanisms and implications. *J. Geophys. Res. Atmos.* **2016**, *121*, 14621-14635.

(28) Berndt, T.; Kaethner, R.; Voigtländer, J.; Stratmann, F.; Pfeifle, M.; Reichle, P.; Sipilä, M.; Kulmala, M.; Olzmann, M. Kinetics of the unimolecular reaction of CH_2OO and the bimolecular reactions with the water monomer, acetaldehyde and acetone under atmospheric conditions. *Phys. Chem. Chem. Phys.* **2015**, *17*, 19862-19873.

(29) Hansel, A.; Scholz, W.; Mentler, B.; Fischer, L.; Berndt, T. Detection of RO_2 radicals and other products from cyclohexene ozonolysis with NH_4^+ and acetate chemical ionization mass spectrometry. *Atmos. Environ.* **2018**, *186*, 248-255.

(30) Kroll, J. H.; Sahay, S. R.; Anderson, J. G.; Demerjian, K. L.; Donahue, N. M. Mechanism of HO_x formation in the gas-phase ozone-alkene reaction. 2. Prompt versus thermal dissociation of carbonyl oxides to form OH. *J. Phys. Chem. A* **2001**, *105*, 4446-4457.

(31) Donahue, N. M.; Kroll, J. H.; Anderson, J. G.; Demerjian, K. L. Direct observation of OH production from the ozonolysis of olefins. *Geophys. Res. Lett.* **1998**, *25*, 59-62.

(32) Zhang, D.; Zhang, R. Ozonolysis of *a*-pinene and *b*-pinene: Kinetics and mechanism. *J. Chem. Phys.* **2005**, *122*, 114308.

(33) Peeters, J.; Vereecken, L.; Fantechi, G. The detailed mechanism of the OH-initiated atmospheric oxidation of α-pinene: a theoretical study. *Phys. Chem. Chem. Phys.* **2001**, *3*, 5489-5504.

(34) Criegee, R. Mechanism of ozonolysis. *Angew. Chem. Int. Ed.* **1975**, *14*, 745-752.

(35) Taatjes, C. A.; Welz, O.; Eskola, A. J.; Savee, J. D.; Scheer, A. M.; Shallcross, D. E.; Rotavera, B.; Lee, E. P.; Dyke, J. M.; Mok, D. K.; Osborn, D. L.; Percival, C. J. Direct measurements of conformer-dependent reactivity of the Criegee intermediate CH_3CHOO. *Science* **2013**, *340*, 177-180.

(36) Drozd, G. T.; Donahue, N. M. Pressure dependence of stabilized Criegee intermediate formation from a sequence of alkenes. *J. Phys. Chem. A* **2011**, *115*, 4381-4387.

(37) Sipilä, M.; Jokinen, T.; Berndt, T.; Richters, S.; Makkonen, R.; Donahue, N. M.; Mauldin III, R. L.; Kurtén, T., Paasonen, P., Sarnela; N., Ehn, M.; Junninen, H.; Rissanen, M. P.; Thornton, J.; Stratmann, F.; Herrmann, H.; Worsnop, D. R.; Kulmala, M.; Kerminen, V.-M.; Petäjä, T. Reactivity of stabilized Criegee intermediates (sCIs) from isoprene and monoterpene ozonolysis toward SO_2 and organic acids. *Atmos. Chem. Phys.* **2014**, *14*, 12143-12153.

(38) Hyttinen, N.; Rissanen, M.P.; Kurtén, T. Computational comparison of acetate and nitrate chemical ionization of highly oxidized cyclohexene ozonolysis intermediates and products. *J. Phys. Chem. A* **2017**, *121*, 2172-2179.

(39) Hyttinen, N.; Otkjær, R.V.; Iyer, S.; Kjaergaard, H.G.; Rissanen, M.P.; Wennberg, P.O.; Kurtén, T. Computational comparison of different reagent ions in the chemical ionization of oxidized multifunctional compounds. *J. Phys. Chem. A* **2018**, *122*, 269-279.

(40) Atkinson, R.; Aschmann, S.M.; Arey, J.; Shores, B. Formation of OH radicals in the gas phase reaction of O_3 with a series of terpenes. *J. Geophys. Res.* **1992**, *97*, 6065-6073.

(41) Hyytinen, N.; Kupiainen-Määttä, O.; Rissanen, M.P.; Muuronen, M.; Ehn, M.; Kurtén, T. Modeling the charging of highly oxidized cyclohexene ozonolysis products using nitrate-based chemical ionization. *J. Phys. Chem. A* **2015**, *119*, 6339-6345.

(42) Kristensen, K.; Cui, T.; Zhang, H.; Gold, A.; Glasius, M.; Surratt, J. D. Dimers in α-pinene secondary organic aerosol: effect of hydroxyl radical, ozone, relative humidity and aerosol acidity. *Atmos. Chem. Phys.* **2014**, *14*, 4201-4218.

(43) Zhao, Y.; Wingen, L. M.; Perraud, V.; Greaves, J.; Finlayson-Pitts, B. J. Role of the reaction of stabilized Criegee intermediates with peroxy radicals in particle formation and growth in air. *Phys. Chem. Chem. Phys.* **2015**, *17*, 12500-12514.

(44) Newland, M. J.; Rickard, A. R.; Sherwen, T.; Evans, M. J.; Vereecken, L.; Munoz, A.; Rodenas, M.; Bloss, W. J. The atmospheric impacts of monoterpene ozonolysis on global stabilized Criegee intermediate budgets and SO_2 oxidation: experiment, theory and modelling. *Atmos. Chem. Phys.* **2018** *18*, 6095-6120.

(45) Welz, O.; Eskola, A. J.; Sheps, L.; Rotavera, B.; Savee, J. D.; Scheer, A. M.; Osborn, D. L.; Lowe, D.; Booth, A. M.; Xiao, P.; Khan, M. A. H.; Percival, C. J.; Shallcross, D. E.; Taatjes, C. A. Rate coefficients of C1 and C2 Criegee intermediate reactions with formic and acetic acid near collision limit: Direct kinetics measurements and atmospheric applications. *Angew. Chem. Int. Ed.* **2014**, *53*, 4547-4550.

(46) Ziemann, P. J.; Atkinson, R. Kinetics, products, and mechanisms of secondary organic aerosol formation. *Chem. Soc. Rev.* **2012**, *41*, 6582-6605.

(47) Atkinson, R. Kinetics and mechanisms of the gas-phase reactions of the hydroxyl radical with organic compounds under atmospheric conditions. *Chem. Rev.* **1986**, *86*, 69-201.

(48) Nguyen, T. B.; Tyndall, G. S.; Crounse, J. D.; Teng, A. P.; Bates, K. H.; Schwantes, R. H.; Coggon, M. M.; Zhang, L.; Feiner, P.; Miller, D. O.; Skog, K. M.; Rivera-Rios, J. C.; Dorris, M.; Olson, K. F.; Koss, A.; Wild, R. J.; Brown, S. S.; Goldstein, A. H.; de Gouw, J. A.; Brune, W. H.; Keutsch, F. N.; Seinfeld, J. H.; Wennberg, P. O. Atmospheric fates of Criegee intermediates in the ozonolysis of isoprene. *Phys. Chem. Chem. Phys.* **2016**, *18*, 10241-10254.

(49) Pöhlker, C.; Wiedemann, K. T.; Sinha, B.; Shiraiwa, M.; Gunthe, S. S.; Smith, M.; Su, H.; Artaxo, P.; Chen, Q.; Cheng, Y.; Elbert, W.; Gilles, M. K.; Kilcoyne, A. L. D.; Moffet, R. C.; Weigand, M.; Martin, S. T.; Pöschl, U.; Andreae, M. O. Biogenic potassium salt particles as seeds for secondary organic aerosol in the Amazon. *Science* **2012**, *337*, 1075-1078.

(50) Kindler-Scharr, A.; Wildt, J.; Dal Maso, M.; Hohaus, T.; Kleist, E.; Mentel, T.F.; Tillmann, R.; Uerlings, R.; Schurr, U.; Wahner, A. New particle formation in forests inhibited by isoprene emissions. *Nature* **2009**, *461*, 381-384.

(51) Stone, D.; Whalley, L.K.; Heard, D.E. Tropospheric OH and HO_2 radical: field measurements and model comparison. *Chem. Soc. Rev.* **2012**, *41*, 6348-6404.

TOC entry

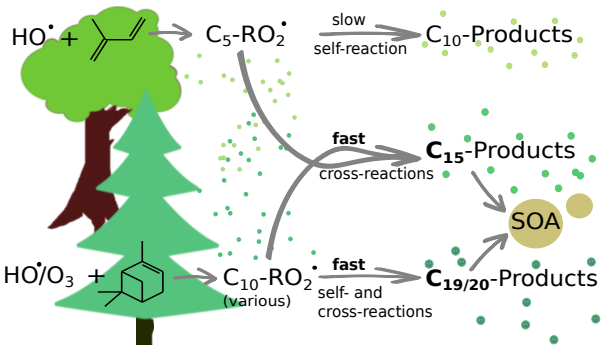
HO• +
C5-RO2•
slow
self-reaction
C10-Products
fast
cross-reactions
C15-Products
SOA
HO•/O3 +
C10-RO2•
(various)
fast
self- and
cross-reactions
C19/20-Products